

1 **Core ideas**

- 2 • 8,778 SNPs and 13 agronomic traits characterized a panel of 423 finger millet landraces.
3 • 4 clusters of accessions coincided with major geographic areas of finger millet cultivation.
4 • A comparison of phenotypic and genomic data indicated a complex diversification history.
5 • This was confirmed by the analysis of allotetraploid finger millet's separate sub-genomes.
6 • Comprehensive new knowledge for intra- and inter-regional breeding is provided.

7
8 **Genomic and phenotypic characterization of finger millet indicates a complex**
9 **diversification history**

10 Jon Bančić^{1,2,*}, Damaris A. Odeny³, Henry F. Ojulong³, Samuel M. Josiah⁴, Jaap Buntjer¹, R.
11 Chris Gaynor¹, Stephen P. Hoad², Gregor Gorjanc¹, Ian K. Dawson²

12 ¹ The Roslin Institute and Royal (Dick) School of Veterinary Studies, University of Edinburgh,
13 Easter Bush Research Centre, Midlothian EH25 9RG, UK

14 ² Scotland's Rural College (SRUC), Kings Buildings, West Mains Road, Edinburgh EH9 3JG,
15 UK

16 ³ International Crops Research Institute for the Semi-Arid Tropics, ICRAF House, UN Avenue,
17 Gigiri, P.O. BOX 39063-00623 Nairobi, Kenya

18 ⁴ University of Georgia, Department of Horticulture, Athens, GA, 30602-7273, USA

19

20 **Abbreviations:** AMOVA, analysis of molecular variance; CV, coefficient of variation; DAPC,
21 Discriminant Analysis of Principal Components; DArTseq, Diversity Arrays Technology
22 sequencing; GRM, genomic relationship matrix; GWAS, genome-wide association study; LD,
23 linkage disequilibrium; MAF, minor allele frequency; MLM, mixed linear model; MTA, marker-
24 trait association; NJ, neighbour-joining; PCA, principal component analysis; RR-BLUP, ridge
25 regression-best linear unbiased genomic prediction; SNP, single nucleotide polymorphism

26

27

ABSTRACT

28

Advances in sequencing technologies mean that insights into crop diversification aiding future

29

breeding can now be explored in crops beyond major staples. For the first time, we use a genome

30

assembly of finger millet, an allotetraploid orphan crop, to analyze DArTseq single nucleotide

31

polymorphisms (SNPs) at the sub-genome level. A set of 8,778 SNPs and 13 agronomic traits

32

characterizing a broad panel of 423 landrace accessions from Africa and Asia suggested the crop

33

has undergone complex, context-specific diversification consistent with a long domestication

34

history. Both Principal Component Analysis and Discriminant Analysis of Principal Components

35

of SNPs indicated four groups of accessions that coincided with the principal geographic areas of

36

finger millet cultivation. East Africa, the considered origin of the crop, appeared the least

37

genetically diverse. A Principal Component Analysis of phenotypic data also indicated clear

38

geographic differentiation, but different relationships among geographic areas than genomic data.

39

Neighbour-joining trees of sub-genomes A and B showed different features which further

40

supported the crop's complex evolutionary history. Our genome-wide association study indicated

41

only a small number of significant marker-trait associations. We applied then clustering to marker

42

effects from a ridge regression model for each trait which revealed two clusters of different trait

43

complexity, with days to flowering and threshing percentage among simple traits, and finger length

44

and grain yield among more complex traits. Our study provides comprehensive new knowledge

45

on the distribution of genomic and phenotypic variation in finger millet, supporting future breeding

46

intra- and inter-regionally across its major cultivation range.

47

INTRODUCTION

48 Diversifying crop production is an important global objective to address human and environmental
49 health concerns, such as malnutrition and the use of intensive unsustainable monoculture
50 production systems (Bančič et al., 2021; von Grebmer et al., 2014). To achieve diversification, we
51 need to increase focus on under-researched crops, also known as orphan crops. Some of these
52 orphan crops are rich in micro- and macro-nutrients and can complement other crops in food
53 production systems, even when farming conditions are adverse (Kamenya et al., 2021; Mustafa et
54 al., 2019). Apart from their intrinsic value, many orphan crops have complex demographic
55 histories that can shed light on broader crop domestication and diversification processes (Meyer
56 & Purugganan, 2013). The high cost of generating genomic resources has however traditionally
57 prevented genomic analyses for orphan crops, but a significant cost-reduction in high-throughput
58 sequencing in the last decade has provided new opportunities for their research (Jamnadass et al.,
59 2020).

60 Finger millet (*Eleusine coracana* (L.) Gaertn. subsp. *coracana*; Poaceae, subfamily Chloridoideae)
61 is an annual small-grained cereal and an orphan crop with an essential role in smallholder food
62 production systems in parts of Africa and Asia. The crop's attractive characteristics include its rich
63 nutritional profile, versatility in food usage, good storage properties, high market value,
64 adaptability to poor production conditions, and flexibility in integrating into various farming
65 approaches (Odeny et al., 2020; Sood et al., 2019). According to de Wet et al. (1984), the
66 allotetraploid crop ($2n=4x=36$; genome constitution AABB, reported disomic inheritance) is
67 thought to have been domesticated from wild *E. coracana* subsp. *africana* in either Uganda or the
68 Ethiopian highlands of East Africa around five millennia ago. The domesticated subsp. *coracana*
69 then spread to southern Africa while broadly maintaining sympatry with the subsp. *africana* wild

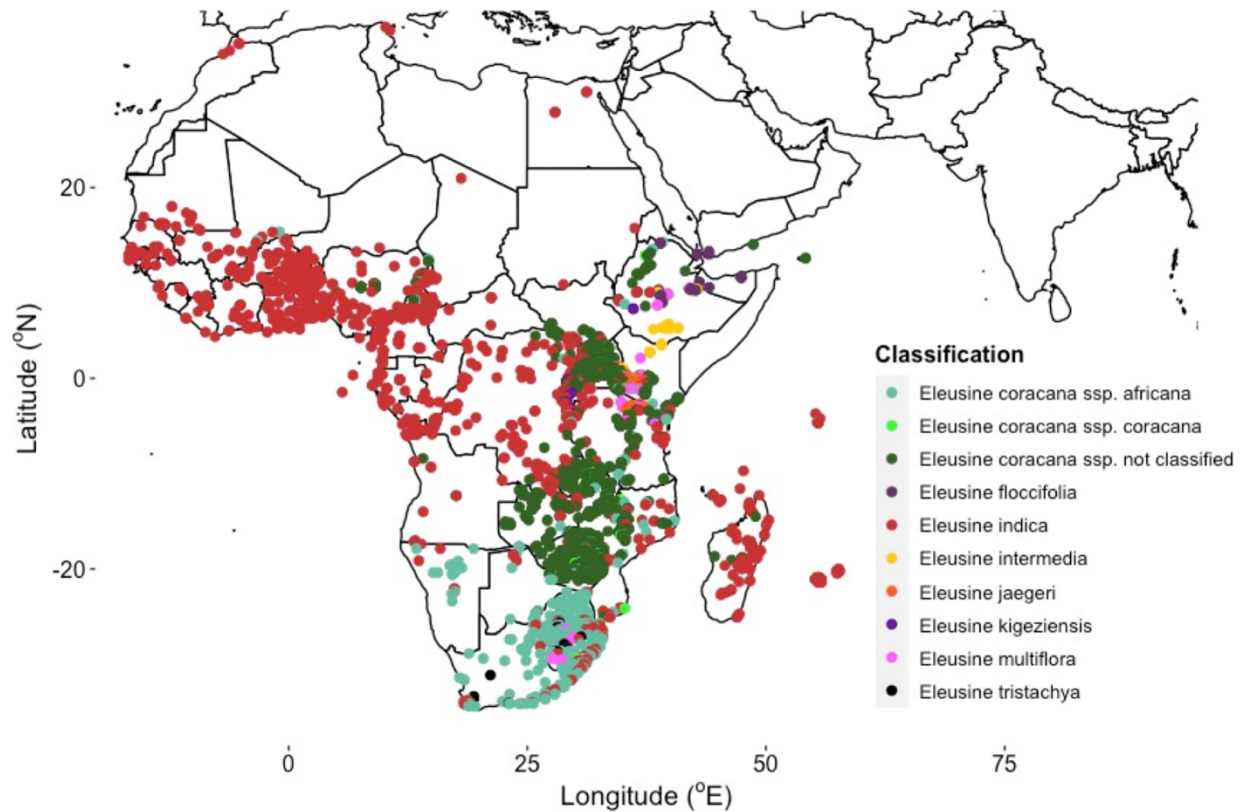
70 form, and remaining in proximity to other *Eleusine* species (see a distribution of the eight *Eleusine*
71 species in Africa depicted in **Fig. 1**). According to de Wet et al. (1984), the crop was introduced
72 to India around three millennia ago, from where it was then dispersed further, including to Nepal.
73 Therefore, East Africa is considered the primary centre of diversity and India an important
74 secondary centre. The immediate wild progenitor of finger millet is believed to have arisen in East
75 Africa by hybridization between two diploid species, the first of which being *E. indica*, which still
76 occurs widely across Africa and is considered the (maternal) donor of what has become finger
77 millet's A sub-genome; and the second, still unknown (and now possibly extinct), diploid pre-B
78 sub-genome donor (Liu et al., 2014; Zhang et al., 2019).

79 In Africa and Asia, subsistence farmers who rely on finger millet mostly grow landrace varieties,
80 and systematic genetic improvement has been limited. This and its complicated biology reflect
81 finger millet's status as an orphan crop. The crop predominantly self-pollinates and has small
82 flowers, which challenges artificial crosses (Dida & Devos, 2006). Moreover, its genomic status
83 as an allotetraploid with an unknown B sub-genome donor has hampered the development of
84 genomic resources. This is because difficulties in distinguishing between sub-genomes and thus
85 the inaccurate calling of homologous versus homeologous single nucleotide polymorphism (SNP)
86 positions are a possibility (Hatakeyama et al., 2018; Hittalmani et al., 2017). Landrace varieties
87 however provide important opportunities to explore crop domestication and diversification. Many
88 have been sampled for conservation in genebanks (Upadhyaya et al., 2006) and these accessions
89 are available for use in breeding programs. They are also a resource to explore the crop's
90 diversification history, a topic that has so far received only limited attention.

91 The recent availability of a draft genome sequence and a robust linkage map for finger millet
92 transform the potential for using genomic information to assist breeding and further understand

Characterization of finger millet

93 the crop's diversification history (Odeny et al., 2020). This paper uses a combination of genomic
94 and phenotypic data to explore a broad panel of 423 finger millet landrace accessions sampled
95 across its main cultivation regions in Africa and Asia. We make use of Diversity Arrays
96 Technology sequencing (DARTseq) (Sansaloni et al., 2011) SNP markers that are, for the first time,
97 placed onto finger millet sub-genomes using the recent genome assembly ([https://phytozome-](https://phytozome-next.jgi.doe.gov/info/Ecoracana_v1_1)
98 [next.jgi.doe.gov/info/Ecoracana_v1_1](https://phytozome-next.jgi.doe.gov/info/Ecoracana_v1_1)). Our objective is to characterize the crop's genomic and
99 phenotypic variation to explore the diversification process and to provide insights for future
100 breeding across its main cultivation range. We here explore multiple features of finger millet
101 variation, including the geographic structuring of genomic and phenotypic diversity, sub-genome
102 specific diversity profiles, germplasm migration events amongst geographic areas, and genetic
103 architecture and selection patterns for agronomic traits. Our analysis provides essential
104 information for the future development of finger millet and is a model for exploring other orphan
105 crops.
106



107 **Fig. 1: Distribution of eight *Eleusine* species across the African continent.** A total of 9,250
108 known locations of *Eleusine* were extracted from the Global Biodiversity Information Facility
109 (GBIF; <https://www.gbif.org/>). Some *Eleusine coracana* entries in GBIF were not classified at the
110 subspecies level ('not classified' in key).
111

111

112

MATERIALS AND METHODS

113

Plant material

114 This study uses the most extensive set of jointly genotyped and phenotyped finger millet landrace
115 accessions to date from the crop's main cultivation regions in Africa and South Asia. The panel
116 initially contained 458 accessions (later reduced to 423 accessions for analysis) that as well as
117 encompassing the main cultivation regions included a small number of accessions collected more
118 widely (**Tab. S1**). In total, 19 accessions (designated as "other") were collected outside the main
119 cultivation regions or are of unknown origin. Our panel is from the ICRISAT genebank's Core

120 Collection of finger millet assembled by Upadhyaya et al. (2006). The 458 accessions are a subset
121 with extensive phenotypic variation and have been the focus of breeder's activities in recent years.
122 Most of the Core Collection was initially sampled directly from farmers' fields, although
123 sometimes accessions were sampled from local markets (see, e.g., Rao, 1980).

124

125 **Collecting and processing genomic data**

126 Leaf tissue was taken from single individuals of each of the 458 accessions, grown in a greenhouse
127 at ICRISAT in Nairobi and dried with silica gel. Genomic DNA (gDNA) was extracted from
128 finely-ground leaf material using the ISOLATE II Genomic DNA Kit (Bioline Pty Ltd) and
129 according to the manufacturer's instructions. The purity and quantity of extracted gDNA was
130 determined by gel electrophoresis and a Qubit 2.0 Fluorometer (Life Technologies, Carlsbad, CA),
131 respectively, with a final dilution of gDNA to 50 ng/μl. Genomic DNA was then delivered to the
132 Integrated Genotyping Service and Support (IGSS) facility at the Bioscience eastern and central
133 Africa–International Livestock Research Institute (BeCA–ILRI) hub in Nairobi. This was for
134 library construction and DArTseq data generation with SNP positions' assignment using the v1.1
135 finger millet genome assembly (https://phytozome-next.jgi.doe.gov/info/Ecoracana_v1_1), and
136 initial output quality control steps, using methods described previously (Sansaloni et al., 2011).

137 The IGSS facility generated 70,906 raw SNPs via DArTseq, which we then quality filtered using
138 TASSEL (version 5.0; Bradbury et al. 2007) as illustrated in **Fig. S1**. The accessions and SNPs
139 were filtered using a minimum call rate of 70%, which reduced our initial sample size of 458
140 accessions to 423 (**Tab. S1**). This constituted our final accession set for later data analyses. We
141 then retained only those SNPs with a minor allele frequency (MAF) > 0.01. In further screening,

142 we removed SNPs with a heterozygosity level greater than $2pq \times (1 - F)$, where p and q are the
143 frequencies of the two allele states, and F is the inbreeding coefficient, for which a value of 0.5
144 was chosen due to the self-pollinating nature of finger millet. This last filter was applied to remove
145 SNP calls that most likely originated from incorrectly collapsing homeologous positions across
146 the two sub-genomes.

147

148 **Measuring linkage disequilibrium decay along chromosomes**

149 Since our analysis is the first to use SNP marker positions assigned using a finger millet genome
150 assembly, we initially explored associations among our high-quality SNP data set in our specific
151 germplasm panel. We calculated linkage disequilibrium (LD) decay (r^2) between all pairwise intra-
152 chromosomal SNP combinations using a full correlation matrix either uncorrected or corrected for
153 bias based on underlying genetic structure across the accessions. Calculations of r^2 were performed
154 in the R package *LDcorSV* (Mangin et al., 2012). Pairwise r^2 values were then plotted against
155 chromosomal physical distance. The decay curve was fitted based on Hill and Weir (1988) using
156 R code from Marroni et al. (2011) and was then used to estimate the distance at which r^2 decreased
157 to 0.2. We estimated LD decay for each chromosome separately, for each sub-genome and for the
158 genome as a whole.

159

160 **Genetic structure, differentiation and diversity**

161 **Genome-wide genetic structure**

162 We used four approaches to characterize and visualize genetic structure. First, we used R packages
163 *ade4* (Dray & Dufour, 2007) and *adeigenet* (Jombart, 2008; the *find.clusters* function) to undertake
164 Principal Component Analysis (PCA) and Discriminant Analysis of Principal Components
165 (DAPC). For the latter, the optimum PC number and cluster number (*k*) were set based on the
166 change in the curve shape of profiles (**Figs. S2, S3**). Second, we constructed a genomic relationship
167 matrix (GRM) using a centred-identity-by-state method (Endelman & Jannink, 2012) in TASSEL.
168 A heatmap of the GRM, calculated using the unweighted pair group method with arithmetic mean
169 (UPGMA) cluster algorithm, was visualized using the *heatmap* R function (R Core Team, 2019).
170 Third, we constructed using TASSEL and plotted with R package *phangorn* (Schliep, 2011) an
171 unweighted neighbour-joining (NJ) tree (Saitou & Nei, 1987) of accessions. We extended NJ
172 analysis to consider not only genome-wide markers but SNPs pooled at the sub-genome level.
173 Fourth, we visualized the country-level geographic distribution of finger millet accessions
174 assigned to their genetic clusters using R packages *rworldmap* (South, 2011) and *ggplot2*
175 (Wickham, 2009).

176 **Detection of introgression and gene flow**

177 We used Treemix (Pickrell & Pritchard, 2012) to infer the most likely evolutionary history and
178 evidence for introgression amongst groups of accessions assigned to four geographic areas of
179 sampling that we term ‘East Africa’, ‘Southern Africa’, ‘India’ and ‘Nepal’ (**Tab. S1**). For
180 simplification, the small number of accessions sampled from countries outside these locations (9
181 of all 404 ‘known’-location accessions) were assigned to the most proximate of our defined four
182 areas (indicated with ellipses in **Fig. 2d**). The 19 accessions designated as “other” (see Plant

183 material section) were excluded from geographic area analysis. **Table S1** provides complete
184 information, but, in brief: the area ‘East Africa’ included a small number of additional accessions
185 (N = 5) from Nigeria and Senegal; and ‘India’ included a few extra lines (N = 4) from Sri Lanka,
186 the Maldives and Pakistan. Using Treemix, maximum-likelihood population trees were
187 constructed based on genome-wide SNPs using blocks of 50 SNPs and ‘East Africa’ rooted as an
188 out-group. The number of tested migration events was varied from zero to three. Bootstrap
189 replicates were generated using 50 SNPs to evaluate the robustness of tree topology, and Treemix
190 R plotting functions were used to visualize results.

191 **Chromosome-level nucleotide diversity and differentiation**

192 We analyzed diversity and differentiation at a chromosome level for both sub-genomes of finger
193 millet for accessions assigned to four geographic areas of sampling (areas as explained above). For
194 each area, we calculated π (Nei and Li, 1979) as our estimator of diversity and pairwise F_{ST} values
195 (Weir and Cockerham, 1984) as our estimator of differentiation, using VCFtools (Danecek et al.,
196 2011) and a 1 Mb non-overlapping sliding window. Genetic differentiation estimates were
197 calculated for all six possible pairwise combinations of geographic areas. Results were plotted
198 against chromosomal positions using R package *ggplot2*.

199 **Summarized gene diversity and differentiation statistics**

200 We summarised genome-wide gene diversity and differentiation for the four geographic areas.
201 Genome-wide gene diversity (H; Nei, 1973) and pairwise F_{ST} values based on all high-quality
202 SNPs were calculated with R package *hierfstat* (Goudet, 2005). We also computed H values for
203 the four defined genetic clusters (see above) of finger millet accessions (these approximate our
204 four defined geographic areas, as will be explained below). We further extended our analysis of

205 geographic areas to consider genome-wide markers and diversity at the sub-genome level. We also
206 used R package *pegas* (Paradis, 2010) for an analysis of molecular variance (AMOVA) that
207 partitioned genetic variation within and among our geographic areas (or clusters) as part of the
208 total panel, based on 100,000 permutations.

209

210

Collecting and analyzing phenotypic data

211 To collect information on phenotypic variation in finger millet, we characterized our initial panel
212 of 458 accessions for 13 life history and other traits (**Tab. S2**) in a field trial that used a complete
213 randomized block design with two replications. The trial was conducted over the long rainy season
214 of 2015 at the Kenya Agricultural and Livestock Research Organization field station at Kiboko in
215 Eastern Kenya (coordinates: 2° 20' N, 37° 45' E; altitude: 960m; annual temperatures: min.
216 16.6°C, max. 29.4°C, average 23.0°; sandy clay loam calcareous soil). Seeds of each accession
217 were drilled in 2 m long plots of two rows spaced 50 cm apart. Within rows, plants were thinned
218 after establishment to a spacing of 10 cm. Five plants for each plot were randomly selected for
219 data recording, though some traits were recorded on a whole plot basis (**Tab. S2**). The traits we
220 measured included features of morphology, physiology and yield that are important for crop
221 production and the integration of finger millet in mixed crop farming systems (Dawson et al.,
222 2019), including in intercrop systems (Brooker et al., 2015), that are of particular interest in
223 breeding research (Bančić et al., 2021).

224 Our analysis of variance of phenotypic data used the following statistical model:

225

$$y_{ikn} = \mu + r_k + g_i + b_{kn} + e_{ikn},$$

Characterization of finger millet

226 where y_{ikn} is generally the average phenotype of five plants of the i^{th} accession tested in the k^{th}
227 replication ($k = 1, 2$) and in the n^{th} block ($n = 1, \dots, n$); μ is the intercept; r_k is the fixed effect of a
228 replication; g_i is the random accession (genotype) effect assuming $g_i \sim N(0, \sigma_G^2)$; b_{kn} is the
229 random block effect assuming $b_{kn} \sim N(0, \sigma_b^2)$; and e_{ikn} is the random residual assuming
230 $e_{ikn} \sim N(0, \sigma_e^2)$. Here $N(., .)$ denotes a normal random variable and σ_G^2 , σ_b^2 and σ_e^2 are respectively
231 variances between accessions, blocks and residuals. We treated accessions as fixed effects to
232 obtain best linear unbiased estimates (BLUEs) for each phenotypic trait. Models were fitted using
233 R package *ASReml-R* (version 4.1.0.90; Butler et al. 2017). We estimated broad-sense heritability
234 across the two replications of the trial ($p = 2$) for each trait as $H^2 = \frac{\sigma_G^2}{\sigma_G^2 + \frac{\sigma_e^2}{p}}$. Distributions of BLUEs
235 for each phenotypic trait and Pearson's correlation coefficients (r ; Pearson, 1895) between all
236 pairwise combinations were calculated and visualized using R (R Core Team, 2019). The
237 coefficient of variation (CV) for each phenotypic trait was calculated as $(\sigma/\bar{x}) \times 100\%$ using
238 BLUEs.

239 We then performed Principal Component Analysis using BLUEs of traits to understand the
240 phenotypic structure in these data using R package *factoextra* (Kassambara & Mundt, 2020).
241 Variation of BLUEs within our defined geographic areas and genetic clusters was also visualized
242 using boxplots.

243

244 **Trait genetic architecture and further genomic-phenotypic comparison**

245 **Genome-wide association analysis**

246 To test each SNP's effect on the 13 phenotypic traits, we ran a genome-wide association study
247 (GWAS) in TASSEL using a linear mixed model that corrected for genetic structure and cryptic
248 relatedness (Yu et al., 2006). BLUEs calculated for each trait were taken as phenotype, and 8,778
249 SNPs were taken as genotype. The model estimated variance components only once using the P3D
250 method. A Bonferroni threshold of 5% was applied to account for multiple testing to declare
251 significant marker-trait associations (MTAs). Manhattan and quantile-quantile (Q-Q) plots of the
252 GWAS results were visualized with R package *qqman* (Turner, 2014). Putative candidate genes
253 were selected using a 25 kb genomic interval both upstream and downstream of a significant MTA.
254 The interval was queried against the current finger millet genome assembly using the Integrated
255 Genomics Viewer (IGV, v. 2.82; Robinson et al., 2011).

256 **Clustering SNP effects**

257 To further evaluate the genetic architecture of the 13 phenotypic traits, we explored the
258 distributions of SNP effects from a ridge regression model (RR-BLUP) (Kooke et al., 2016).
259 BLUEs calculated for each trait scaled by their standard deviation were taken as phenotype, and
260 an imputed 8,778 SNP matrix were taken as genotype. A *k*-nearest neighbour imputation of the
261 SNP matrix was performed in TASSEL using default parameters and RR-BLUP models were fitted
262 in R package *AlphaMME* (<https://github.com/gaynor/AlphaMME>). SNP effects from the RR-
263 BLUP model were then used to: first, calculate pairwise Euclidean distances over the first five
264 mathematical moments in R package *moments* (v0.14; Komsta and Novomestky, 2011); and,
265 second, construct a dendrogram from the Euclidean distance matrix using the UPGMA cluster
266 algorithm with the *hclust* R function (R Core Team, 2019).

267 **Comparison of phenotypic and genome-wide gene diversity by geographic area**

268 A simple yet useful way to shed light on the particular selection histories of crops as they take
269 different diversification pathways within specific geographic contexts is to compare phenotypic
270 diversity levels with levels of underlying genome-wide gene diversity. Here, we adopt a
271 straightforward approach for initial comparisons that involves individual phenotypic trait CV
272 values and gene diversity (H) values for genome-wide SNP data. We calculate CV/H as the
273 comparator for each of our four defined geographic areas to check primarily for rank differences
274 across areas that may indicate particular phenotypic selection pressures by area. This type of
275 approach is exemplified classically in studies of the diversification of tomato, where high
276 phenotypic variation observed at specific traits is accompanied by overall underlying genomic
277 diversity bottlenecks (Rodríguez et al., 2011).

278 **RESULTS**

279 **Genome-wide SNP data cover the entire finger millet chromosome complement but occur**
280 **at a higher density in the A sub-genome**

281 The IGSS facility generated 70,906 raw SNPs, which were filtered into a final marker set of 8,778
282 SNPs for 423 accessions for subsequent analyses. Eight thousand and ninety-six (8,096) SNPs out
283 of the 8,778 had been previously mapped to chromosomes (**Tab. S3**). Initial analysis showed that
284 the full complement of finger millet chromosomes was covered but that chromosome-level SNP
285 density was higher for the A sub-genome (**Tab. 1**; approx. twice the density of markers of the B
286 sub-genome). Across both sub-genomes, the mean SNP density was ~8.6 per Mb. Consistent with
287 expectations of significantly lower recombination in central chromosomal regions of selfing
288 cereals (e.g., Bustos-Korts et al., 2019); SNP density was generally considerably higher toward
289 the ends of chromosomes (**Figs. S4, S9c**). The proportion of markers removed from our initial raw

290 data due to likely being homeologous was a relatively high 3.9% (2,733 out of 70,906; markers
291 above the red curve in **Fig. S1e**). Therefore, precautions with homeologous markers are indicated
292 for finger millet. The observed heterozygosity for the markers in our final set of 8,778 SNPs was
293 very low (median 0.048 and mean 0.057; **Tab. S3**), indicating that most finger millet accessions
294 are highly inbred.

295 **Linkage disequilibrium decay along chromosomes shows expected patterns for both sub-** 296 **genomes**

297 Our work is the first that has used a finger millet genome assembly to assign physical SNP
298 positions for a broad accession panel, so understanding patterns of LD in A and B sub-genomes is
299 of particular relevance. Our calculations indicated the expected overall pattern of LD decay and
300 the importance of correcting for underlying genetic structure among accessions. For the genome
301 as a whole, r^2 decayed to 0.2 at a distance of 106 kb when correcting for genetic structure
302 (compared to a distance of 1.77 Mb for the naïve model). Decay was slower for the B sub-genome
303 ($r^2 = 0.2$ at 168 kb, with correction) than the A sub-genome ($r^2 = 0.2$ at 88 kb), and varied markedly
304 across chromosomes within sub-genomes (**Fig. S5**). Overall, the relatively slow rate of LD decay
305 was consistent with other self-pollinating crops (Flint-Garcia et al., 2003), including other millets
306 (Jaiswal et al., 2019).

307

308 **Tab. 1. Distribution of SNPs by finger millet chromosomes.** SNP density per chromosome was
309 calculated for individual 1 Mb non-overlapping windows as shown in **Figs. S4** and **S9c**.
310

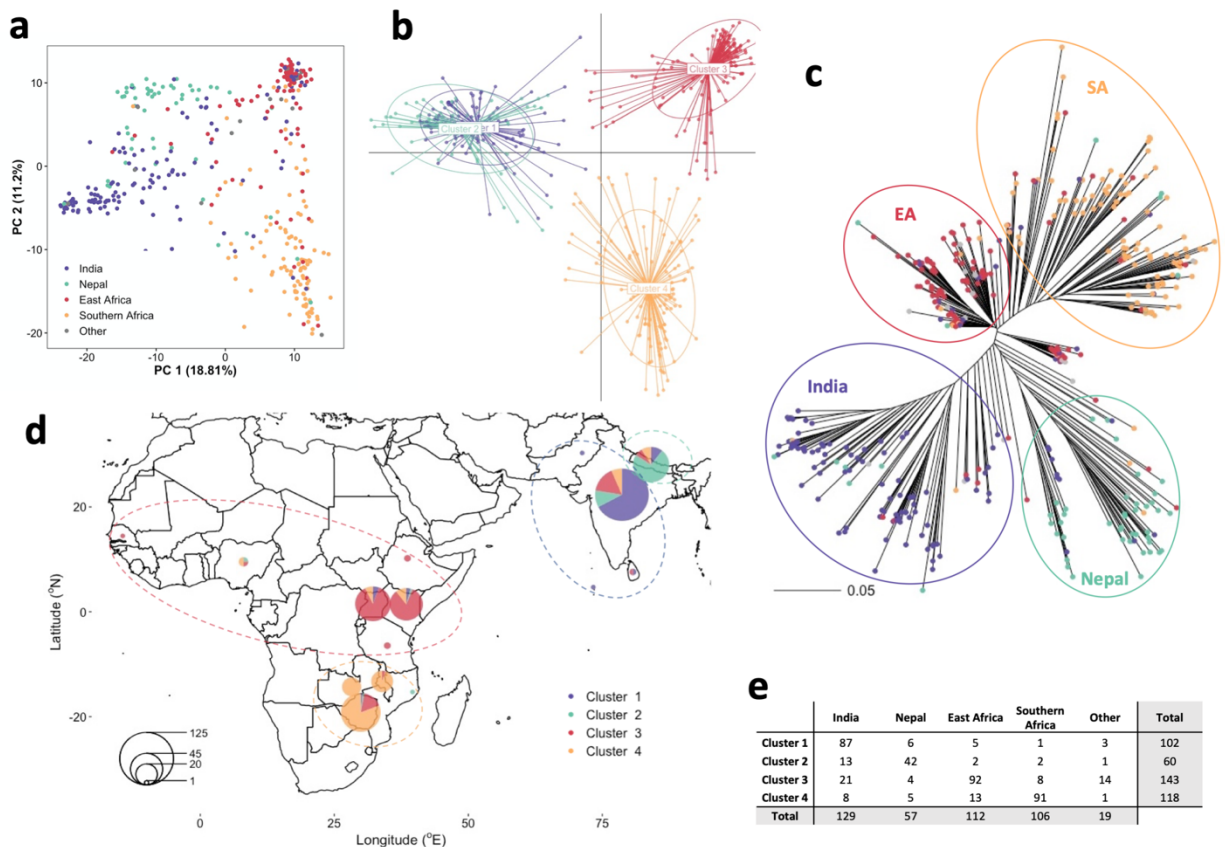
| Chromosome | Number of SNPs | Chromosome length (Mb) | SNP density (per Mb) |
|---------------------|----------------|------------------------|----------------------|
| 1A | 742 | 57.13 | 12.4 |
| 2A | 683 | 60.90 | 11.1 |
| 3A | 570 | 53.87 | 10.9 |
| 4A | 618 | 39.68 | 15.4 |
| 5A | 1057 | 66.30 | 15.4 |
| 6A | 357 | 59.47 | 5.9 |
| 7A | 553 | 48.45 | 11.2 |
| 8A | 307 | 47.22 | 7.6 |
| 9A | 486 | 45.36 | 11.6 |
| Sub-genome A | 5,373 | 53.15 | 11.3 |
| 1B | 196 | 72.49 | 3.7 |
| 2B | 323 | 70.83 | 5.3 |
| 3B | 136 | 63.91 | 2.9 |
| 4B | 158 | 50.88 | 2.9 |
| 5B | 659 | 80.22 | 7.8 |
| 6B | 244 | 74.22 | 5.0 |
| 7B | 267 | 58.85 | 7.1 |
| 8B | 294 | 60.62 | 5.4 |
| 9B | 446 | 62.05 | 7.4 |
| Sub-genome B | 2,723 | 65.20 | 5.7 |
| Scaffolds | 682 | | |
| Whole genome | 8,778 | 1072.44 | 8.6 |

311

312 **Genome-wide genetic structure reveals strong geographic differentiation**

313 Our analysis of genome-wide genetic structure in finger millet revealed clear differentiation
314 patterns (**Fig. 2**). Both PCA and DAPC analyses (DAPC using an optimum principal component
315 number PC = 4 according to **Fig. S2** and an optimal cluster number $k = 4$ according to **Fig. S3**)
316 revealed a genetic structure that corresponded with the four sampled geographic areas of finger
317 millet cultivation (**Fig. 2a, b, d**). Accessions from Africa and Asia regions were separated along
318 the first PC, which explained 18.8% of the total variation, while the second PC, which explained

319 11.2% of the total variation, discriminated between geographic areas within the two continents
 320 (**Fig. 2a**). The overlap between genetic clusters and geographic areas was particularly strong in
 321 Africa (**Fig. 2e, Tab. S4**). The clear overall geographic structuring of genetic variation, with a
 322 degree of admixture, was also evident in our NJ tree (**Fig. 2c**), on the map of sampled geographic
 323 areas showing accessions' assignments to genetic cluster groups (**Fig. 2d**), and in a heatmap of
 324 GRM with UPGMA clustering (**Fig. S6**). The more extensive admixture of finger millet in Asia
 325 than Africa, most clearly observed in **Fig. 2d**, is consistent with more formal breeding of the crop
 326 in Asia, supported by cross-regional germplasm transfer. For example, in India, an improvement
 327 program initiated in the 1960s involved crosses between African and Asian accessions, resulting
 328 in 'Indaf' varieties (Mirza & Marla, 2019; see more in next section). In further NJ analysis that
 329 considered SNPs for sub-genomes A and B separately, clear geographic structuring of genetic
 330 variation was evident in both cases (**Fig. S7**).



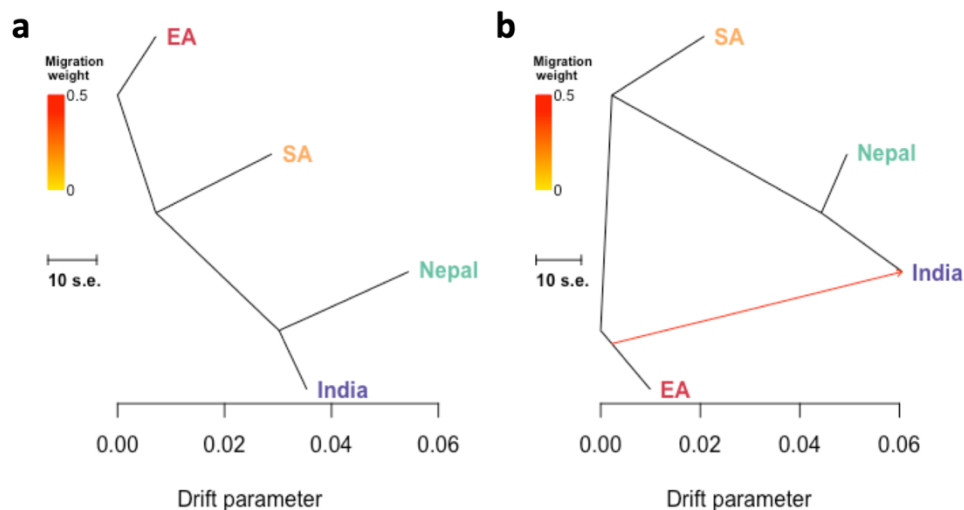
331 **Fig. 2: Geographical distribution and genetic structure of 423 finger millet accessions.** **a,**
332 Score plot using the first two principal components (PCs) illustrates the genetic structure of finger
333 millet coloured according to geographic areas. **b,** Genetic clusters identified by DAPC and
334 coloured according to their corresponding geographic area in **d**). **c,** A phylogenetic neighbour-
335 joining tree with tips coloured by geographic area and enclosing circles representing generalized
336 clades. **d,** Geographical distribution of accessions with pie chart size representing the number of
337 accessions collected in a particular country and slice size representing the probability of belonging
338 to a specific genetic cluster. Dotted ellipses indicate the extent of our applied geographic areas
339 (drawing in small groups of outliers; see Materials and Methods and **Tab. S1** for further
340 information on geographic area assignments). **e,** A table of accessions assigned to geographic areas
341 and genetic clusters; accessions without known location are designated as ‘Other’.

342

343 Genetic introgression and gene flow analysis suggests a migration event between East

344 Africa and India

345 Our Treemix analysis of past admixture events in finger millet suggested a potential historic
346 introgression from East Africa to India. Using ‘East Africa’ as an out-group, the maximum-
347 likelihood tree without migration events (**Figs. 3a** and **S8a**), accounting for drift alone,
348 corresponded to the phylogenetic tree (see **Fig. 2c**). When migration events were allowed, a single
349 event from ‘East Africa’ to ‘India’ was inferred (**Figs. 3b** and **S8b**). These results are consistent
350 with the cultivated finger millet’s demographic history as previously speculated by non-genomic
351 analysis approaches (de Wet et al., 1984; Hilu & de Wet, 1976). These findings are also consistent
352 with known breeding introductions from Africa to Asia (see previous section).



353 **Fig. 3: Inferred finger millet maximum-likelihood population trees with admixture events.**
354 The structure of the graphs inferred by Treemix for four geographic areas of finger millet. **a**, with
355 no migration events. **b**, with one migration event. The migration arrow is coloured according to its
356 weight and represents the fraction of ancestry derived from the migration edge. Horizontal branch
357 lengths are proportional to the amount of genetic drift that has occurred on the branch. The scale
358 bar shows ten times the average standard error (s.e.) of the accessions in the sample. The residual
359 fit from the graph is shown in **Fig. S8**.

360

361 **Chromosome-level nucleotide diversity and differentiation profiles vary by region**

362 Our analysis of nucleotide diversity (π) along chromosomes showed differences in relative
363 diversity for geographic areas by chromosome, including for homeologous (A and B sub-genome)
364 chromosomes (**Fig. S9a**). Notable was relatively high diversity along chromosome 1A for ‘Nepal’
365 (not seen on chromosome 1B) and along chromosomes 5B and 9B for ‘Southern Africa’ (not seen
366 on chromosomes 5A and 9A). Pairwise chromosome-level F_{ST} values for geographic areas (**Fig.**
367 **S9b**) reflected these different diversity profiles, again indicating chromosome-specific, sub-
368 genome-based differences. Of note was high differentiation between both of our African
369 geographic areas and both our Asian geographic areas along chromosome 5A that was not
370 replicated on chromosome 5B.

371 **Summarized gene diversity statistics confirm regional differentiation and sub-genomic** 372 **differences**

373 Our calculation of genome-wide gene diversity (H) values indicated that the ‘Nepal’ region
374 contained the most diversity and the ‘East Africa’ region the least (**Tab. 2**). The ranking of
375 diversity levels corresponded when the analysis was repeated based on genetic clusters that
376 approximate geographic areas. Estimates were, as expected, overall lower when based on genetic
377 clusters, as the most prominent within-area genetic admixture has in this case been reassigned (see
378 **Fig. 2**).

379 Pairwise F_{ST} values summarised for genome-wide SNPs (**Tab. S5**) confirmed our PCA and DAPC
380 results (**Fig. 2a, b, d**), which revealed primary geography-based partitioning between Africa and
381 Asia and then between areas within these regions. The highest differentiation was between
382 ‘Southern Africa’ and ‘Nepal’ accessions ($F_{ST} = 0.167$). Our two AMOVA analyses revealed that
383 16% of total genome-wide variation partitioned among our four geographic areas and 24% among
384 our corresponding but genetically-defined clusters ($p \leq 0.001$ that no structuring in both cases).

385 In the case of gene diversity (H) calculations, we also analyzed geographic areas for separate A
386 and B sub-genomes (**Tab. 2**). The ranking of diversity by geographic area varied for the two sub-
387 genomes, with ‘Nepal’ (still, compared to the entire genome) ranking highest for the A sub-
388 genome but ‘Southern Africa’ highest for the B sub-genome; ‘East Africa’ consistently ranked
389 lowest. The observed diversity ranking change is reflected in the relative spread of accessions from
390 each geographic area in sub-genome NJ trees (**Fig. S7**). It appears to be based on changes in
391 relative diversity for specific pairs of homeologous chromosomes (**Fig. S9a**), notably
392 chromosomes 5B versus 5A, and 9B versus 9A (diversity relatively high at 5B and 9B for
393 ‘Southern Africa’; see also above).

394

395 **Tab. 2. Characterization of gene diversity (H).** Genome-wide measurement of finger millet gene
 396 diversity was undertaken for four geographic areas (left value) and corresponding genetic clusters
 397 identified by DAPC analysis (right value). The values presented for individual sub-genomes are
 398 for geographic areas only. The total sample size for genome-wide estimates varies because of the
 399 non-assignment of some accessions to geographic areas (see Materials and Methods). The area or
 400 cluster with highest diversity is underlined.

| Geographic area / Genetic cluster | Sample size | H | | |
|--------------------------------------|----------------|----------------------|-----------------|-----------------|
| | | Genome- wide | Sub-genome A | Sub-genome B |
| India / Cluster 1 | 129 / 102 | 0.259 / 0.215 | 0.293 | 0.212 |
| Nepal / Cluster 2 | 57 / 60 | <u>0.282 / 0.265</u> | <u>0.336</u> | 0.252 |
| EA / Cluster 3 | 112 / 143 | 0.199 / 0.179 | 0.200 | 0.208 |
| SA / Cluster 4 | 106 / 118 | 0.260 / 0.252 | 0.230 | <u>0.368</u> |

407 Significant variation in phenotypic traits partitions by region

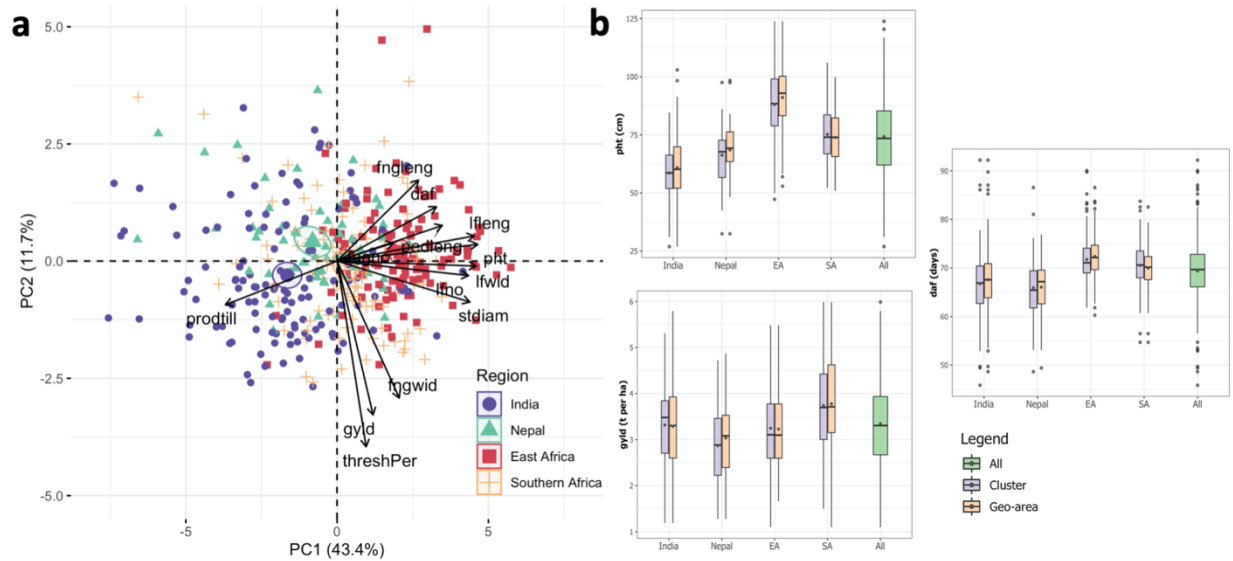
408 Our analysis of 13 phenotypic traits for 423 finger millet accessions revealed extensive variation
 409 (CV from 8.58 for threshing percentage to 48.25 for productive tiller number) and medium-to-high
 410 H^2 values (from 0.35 for grain yield to 0.95 for days to flowering). The level of variation detected
 411 and heritability values were generally consistent with the crop's previous field trials (e.g., Bharathi,
 412 2011; Manyasa et al., 2016).

413 Summary statistics are presented in **Tab. S6**, and trait distributions and between-trait correlations
 414 in **Fig. S10**. The strongest positive correlation was between leaf length and plant height ($r = 0.83$,
 415 $p < 0.001$), and the strongest negative correlation between leaf width and the number of productive
 416 tillers ($r = -0.64$, $p < 0.001$). Considering the three key traits of grain yield, plant height and days
 417 to flowering, a medium-level positive correlation was observed between plant height and days to
 418 flowering ($r = 0.50$, $p < 0.001$), a moderate positive correlation between plant height and grain
 419 yield ($r = 0.19$, $p < 0.001$), and no correlation between days to flowering and grain yield ($r < 0.01$,

420 NS). Principal component analysis using BLUEs of traits further illustrated the levels of
421 correlation between different traits (**Fig. 4a**).

422 Similar to genomic data, we used PCA scores of 404 accessions to examine our phenotypic data
423 structure. Confidence ellipses based on geographic areas (**Fig. 4a**; confidence level set to 95%
424 around area centroid) indicated a degree of separation along the first PC for all four geographic
425 areas based on combined phenotypes, most clearly separating ‘India’ and ‘East Africa’. Accessions
426 from ‘Nepal’ and ‘Southern Africa’ were relatively less differentiated compared to using genome-
427 wide SNP data (see, e.g., F_{ST} values, **Tab. S5**). Trait-specific boxplots of phenotypic variation by
428 region or genetic cluster (**Fig. 4b** and **Fig. S11**) illustrated a divergent pattern for some traits. For
429 example, for plant height ‘India’ and ‘East Africa’ (or their corresponding clusters) showed the
430 most difference, while for grain yield ‘Nepal’ and ‘Southern Africa’ did. On the other hand, for
431 days to flowering, the greatest difference was between ‘Nepal’ and ‘East Africa’.

432 Of the three last-mentioned traits, only plant height showed non-overlap between areas/clusters
433 (for ‘East Africa’ vs. some other areas/clusters, where ‘East Africa’ accessions were, for example,
434 on average 32% taller than accessions from ‘India’, **Fig. 4b**; the same non-overlap applied for the
435 traits of leaf length, leaf number, leaf width [all greatest for ‘East Africa’] and number of
436 productive tillers [fewest for ‘East Africa’], **Fig. S11**). In general, phenotypes were more
437 differentiated between regions (Africa vs. Asia) than among geographic areas within regions,
438 corresponding to genomic differentiation (**Fig. 2**) and consistent with combined phenotype
439 centroids in **Fig. 4a**. Overall, each geographic area contained extensive phenotypic variation, with
440 India containing the largest (**Tab. S7**). This is also be seen in the PCA and the boxplots (**Figs. 4**
441 **and S11**).



442 **Fig. 4: Summary of phenotypic data for 423 finger millet accessions.** **a**, The Principal
 443 component analysis (PCA) biplot shows vectors of each of the 13 phenotypic traits/variables (black
 444 arrows) and the PCA scores for combined phenotypes of 404 accessions (represented by points)
 445 coloured according to geographic areas; scores of accessions (19) without known location were
 446 excluded. The magnitude of the vectors shows the strength of their contribution to each PC. Vectors
 447 pointing in similar directions indicate positively correlated traits, vectors pointing in opposite
 448 directions indicate negatively correlated variables, and vectors at approximately right angles
 449 indicate low or no correlation. Coloured ellipses represent 95% confidence intervals around the
 450 centroid (bold symbol) for each area. *stdiam*, stem diameter; *lfeng*, leaf length; *lfwid*, leaf width;
 451 *lfno*, leaf number; *fngleng*, finger length; *fngwid*, finger width; *fngno*, finger number; *pedleng*,
 452 peduncle length; *pht*, plant height; *prodtil*, production tillers; *daf*, days to flowering; *thershPer*,
 453 threshing percentage; *gyld*, grain yield. **b**, Boxplots of the statistical distribution of individual trait
 454 values divided according to genetic clusters identified by Discriminant Analysis of Principal
 455 Components (purple boxplots), geographic areas (orange boxplots) and the total phenotypic
 456 variation (green boxplots). The middle bar and the point inside each boxplot represent median and
 457 mean, respectively. Examples are given for days to plant height (*pht*) and grain yield (*gyld*). Results
 458 for the other 10 phenotypic traits are shown in **Fig. S11**.

459

460 **Genome-wide association analysis reveals a small number of significant associations and a**
 461 **range of candidate genes**

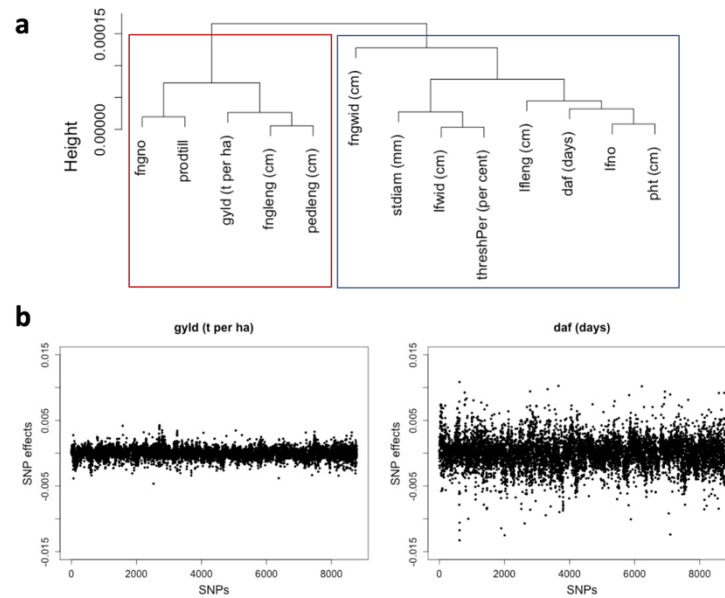
462 Our GWAS detected 16 MTAs above the stringent Bonferroni threshold ($-\log_{10}(0.05/8,778) =$
 463 5.24), 15 of which were chromosome-located. Twelve were associated with finger length (seven
 464 on chromosome 2B, three on 5B, one on 7B and one on 8B), two with days to flowering (one on
 465 4B and one scaffold marker) and two with threshing percentage (one each on 4B and 6B).

466 Manhattan and Q-Q plots for all 13 phenotypic traits are presented in **Fig. S12** and a list of all
467 significant MTAs is given in **Tab. S8**. Most of the SNPs with significant MTAs that we identified
468 by GWAS had a low MAF, in correspondence with our overall SNP panel (MAF < 0.2 for > 75%
469 of all SNPs; see **Fig. S1d**). Therefore, care should be taken when interpreting our findings. The
470 relatively small number of MTAs we detected could reflect the overall limited number of SNPs
471 generated with the current genotyping strategy. All of the significant MTAs that we did detect
472 were associated with the B sub-genome, even though it had a lower SNP density than the A sub-
473 genome (but the B sub-genome does have slower LD decay, see above). A list of 61 unique
474 putative candidate genes revealed within a 25 kb interval both upstream and downstream of
475 significant MTAs is given in **Tab. S8**, but we do not here explore these associations further.

476 **SNP effects clustering demonstrates different genetic architectures of phenotypic traits**

477 Our exploration of SNP effects for phenotypic traits from RR-BLUP revealed two clusters of traits
478 of different levels of complexity (**Fig. 5** and **Fig. S13**). Among traits with simpler genetic
479 architecture were days to flowering and threshing percentage (consistent with the small number of
480 MTAs detected for these two traits, see above). These are traits that do not follow a uniform
481 distribution. Included among the traits with more complex genetic architecture (and of more
482 uniform distribution) were finger length (which did still reveal MTAs in GWAS analysis) and
483 grain yield (no MTAs in our analysis and known in other cereals to be highly polygenic; e.g., for
484 wheat, see Brinton & Uauy, 2019).

Characterization of finger millet

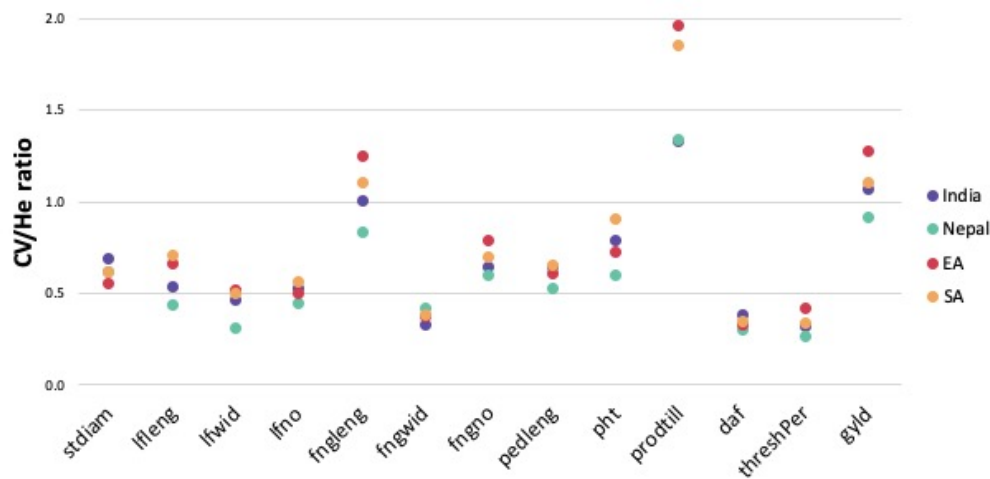


485 **Fig. 5: Clustering of SNP effects obtained from RR-BLUP to determine the complexity of**
486 **agronomic traits. a**, The UPGMA clustering algorithm was applied to the five statistical moments
487 of SNP effects for all 13 agronomic traits. The cluster in red consists of traits with highly polygenic
488 genetic architecture, and the cluster in blue consists of traits with simple- to moderately-complex
489 genetic architecture. **b**, Examples of SNP effect distributions for the complex trait of gyld (grain
490 yield) and the less complex trait daf (days to flowering). The results for the remaining 11 of the
491 individual traits evaluated are shown in **Fig. S13**.
492

493 **Comparison of phenotypic and genome-wide gene diversity by geographic area supports** 494 **varied post-domestication diversification pathways for finger millet**

495 Our geographic-area-based comparison of phenotypic trait diversity with overall underlying gene
496 diversity was based on the calculation of CV/H (i.e., standardized phenotypic variation per unit of
497 genome-wide gene diversity; **Fig. 6**). The results showed that the ranking of values between
498 geographic areas varied by trait, suggesting complex, context-specific diversification of the crop.
499 The comparison of rankings of CV/H for finger number and plant height, for example, showed
500 that the highest rank for the former was for ‘East Africa’ and for the latter was ‘Southern Africa’.
501 Considering all 13 phenotypic traits, ‘East Africa’ most often of any geographic area ranked top
502 for CV/H (in 6 cases) and ‘Nepal’ bottom (11 cases). This is consistent with the relatively low

503 denominator (H) value for ‘East Africa’ compared to ‘Nepal’ (see above), and possibly indicates
504 an ‘overexpression’ of phenotypic variation in the former region that is consistent with a longer
505 domestication history. Days to flowering was the trait with the least spread in CV/H values for
506 geographic areas, indicating that variation in this trait may be the best phenotypic proxy of
507 underlying genomic diversity within geographic areas.



508 **Fig. 6 The ratio of the coefficient of phenotypic variance (CV) and genome-wide gene**
509 **diversity (H) for 13 agronomic traits for four geographic areas. We used the ratios to inform**
510 **us of finger millet’s selection history.**

511

512

DISCUSSION

513 Broadening crop production requires more focus on orphan crops. Orphan crops have an intrinsic
514 value, but they can also provide broader lessons on crop domestication and crop diversification
515 pathways (Dawson et al., 2019). Here, we have studied the orphan crop finger millet and have
516 shown that a combination of modern and traditional methods can provide important insights
517 relevant for the future development of the crop. Our approach also provides a model for work on
518 other orphan crop species.

Characterization of finger millet

519 Past DNA-based studies of finger millet genetic diversity have generally been limited in scope,
520 involving < 150 accessions and/or < 100 polymorphic loci. These studies include those of Dida et
521 al. (2008), Arya et al. (2013), Manyasa et al. (2015), Ramakrishnan et al. (2016), Babu et al.
522 (2018), Lule et al. (2018) and Pandian et al. (2018) who all applied simple sequence repeat (SSR)
523 markers; and those of Gimode et al. (2016) and Sood et al. (2016) who used SSRs and SNPs.
524 Despite their limited scope, these previous studies revealed a degree of locally- and regionally-
525 structured genetic variation, including between Africa and Asia, and admixture between the two
526 continents.

527 A restricted number of previous studies have also sought to explore marker-trait associations in
528 finger millet. However, again the accessions and/or molecular markers involved were generally
529 limited to small numbers, and studies did not have available a finger millet genome assembly to
530 map markers to chromosome positions. These studies include those of Dida et al. (2021) who used
531 a medium-sized panel of SNPs but only 52 East African accessions to search for blast disease
532 resistance MTAs; Puranik et al. (2020) who used a large panel of SNPs but assessed only 190
533 genotypes to search for grain nutrient-content-related MTAs; Sharma et al. (2018) who applied a
534 medium-sized panel of SNPs to only 113 accessions to search for MTAs in 14 agro-morphological
535 traits; and Tiwari et al. (2020) who, beginning with the same SNPs and germplasm panel of Sharma
536 et al. (2018), explored marker associations with grain protein content. Despite their limited scope,
537 these previous studies indicated some MTAs. These were identified under varying degrees of
538 stringency and certainty levels, applying for example candidate gene sequence homologies for
539 characterization.

540 Our analysis was based on both an extensive germplasm panel and a broad genome-wide (and sub-
541 genome-located) SNP marker set. This was combined with extensive field phenotypic assessment,

542 the use of a finger millet genome assembly, and the application of a suite of population genomic
543 tools. Overall, this provides us with a more complete picture than has been possible previously of
544 genetic variation in the finger millet crop. Our analysis supports previous studies that have
545 identified geographically-structured variation. However, it also sheds more light on the apparently
546 complex evolutionary history of finger millet and its varied within and between region
547 diversification pathways, thereby providing new information to support future breeding. Below,
548 we focus further discussion on two aspects of particular interest that expand our current
549 understanding of finger millet: i) polyploidy and sub-genome-specific diversification; and ii)
550 geographically-specific relationships between phenotype and genotype embracing chromosome-,
551 sub-genome-, and genome-level diversity, with a range of individual phenotypic traits and
552 combinations of traits.

553 **Sub-genome-specific diversification and polyploidy**

554 Hybridization between different genomes, followed by chromosome doubling to generate
555 polyploids, has played a crucial role in cereal crop evolution (Levy & Feldman, 2002). This has
556 been well studied for major cereals such as allohexaploid wheat (Feldman & Levy, 2012).
557 However, the full origin of the finger millet allotetraploid genome is not well understood (Zhang
558 et al., 2019). The allopolyploidization event from diploid A and B sub-genome progenitors to form
559 the tetraploid crop ancestor (*E. corocana* subsp. *africana*) is believed to have occurred in East
560 Africa (de Wet et al., 1984). Traditionally, such polyploidization events are thought to be rare in
561 plant's histories and initially lead to genomic bottlenecks in the derived organisms (Stebbins,
562 1950). In the current study, we could not compare relative diversity levels of the cultivated finger
563 millet with the descendants of its wild tetraploid progenitor or previous diploid progenitors.
564 However, previous studies found genomic diversity in cultivated finger millet to be significantly

565 lower than in wild *E. coracana* subsp. *africana* (e.g., Gimode et al., 2016). We were nevertheless
566 able to explore for the first time in finger millet the sub-genomic and chromosome-specific
567 diversity patterns in the crop by geographic area of sampling, which may inform on its evolution.
568 We detected the highest level of genetic diversity in the B sub-genome overall in ‘Southern Africa’,
569 with exceptionally high diversity levels along two chromosomes (5B and 9B). In contrast, for the
570 A sub-genome, ‘Southern Africa’ only ranked third in diversity, while diversity for ‘East Africa’
571 ranked lowest for both sub-genomes.

572 Our new observations are consistent with broadening of diversity in specific parts of the finger
573 millet genome as the crop developed new adaptations during expansion from East Africa to new
574 areas in Africa and in Asia. This may have been facilitated by the polyploidization process that
575 enables mechanisms such as inter-genomic transfer through translocation, recombination, and
576 transposition to support rapid evolution (as outlined by Levy & Feldman, 2002). Our results could
577 also indicate a secondary contact in the ‘Southern Africa’ region between the crop and its
578 immediate progenitor, or perhaps new introgressions from other co-located *Eleusine* species that
579 have specifically targeted the B sub-genome and could have been aided by polyploidization. Both
580 wild *E. coracana* subsp. *africana* (i.e., the considered most likely immediate progenitor) and a
581 range of other *Eleusine* species are sympatric with the finger millet crop in southern Africa (**Fig.**
582 **1**), providing opportunities for introgression. This type of process has been observed in other
583 cereals, including wheat (He et al., 2019), and would be consistent with genotyping-by-sequencing
584 in finger millet that has revealed chromosomal rearrangements between sub-genomes (Qi et al.,
585 2018). Regardless of the cause, the patterns of sub-genome-specific diversity observed in our study
586 suggest complexity in finger millet’s evolution. Genomic exploration of *Eleusine* germplasm panels

587 containing extant descendants of the known and putative crop wild progenitors may further
588 elucidate this complex demographic history.

589 **Region-specific genomic-phenotypic relationships**

590 Our analysis shows complex relationships between genomic and phenotypic variation in finger
591 millet across the four geographic areas we sampled. This is consistent with a crop that has been
592 subject to millennia of domestication and has experienced different selection pressures based on
593 particular human preferences and production environments in different locations. Complex
594 relationships between genetic variation and phenotypic variation are common in crops (e.g., Kozak
595 et al., 2011), and our results were therefore not unexpected.

596 Our analysis of genetic diversity along sub-genomic chromosome homeologs indicated differences
597 in relative diversity for particular geographic areas. The subsequent pooling of chromosome
598 diversity at the sub-genome level also revealed different diversity rankings by location. When
599 levels of geographic-area-based phenotypic variation were compared with genome-wide gene
600 diversity (through the calculation of CV/H), the results suggested context-, trait-, and trait-
601 combination-specific diversification pathways for the crop. In addition, the ‘East Africa’ area most
602 often ranked top for CV/H values, consistent with a longer cultivation history here than elsewhere.
603 The profiles of phenotypic traits alone that varied between geographic areas by individual trait
604 further suggest multiple selection pressures both between and within areas, with the broad
605 variation often captured within areas indicating local differential selection.

606 Finally, patterns of differentiation between geographic areas also varied for genomic data
607 compared to phenotypic data, further supporting complex demographic processes. For example,
608 genome-wide SNPs revealed the highest differentiation between ‘Southern Africa’ and ‘Nepal’

609 accessions, but combined phenotypic data indicated the greatest level of difference between ‘India’
610 and ‘East Africa’. This perhaps illustrates that these last two areas are the strongest foci for context-
611 specific crop development and/or are most agro-ecologically differentiated.

612 **Concluding remarks**

613 This study has revealed distinct genomic and phenotypic variation patterns in finger millet that
614 suggest complex diversification pathways for the crop. Our data provide a firmer basis for the
615 future development of finger millet. The information can, for example, help guide the
616 determination of heterotic groups to produce potentially hybrid finger millet varieties in the future
617 (Labroo et al., 2021; Mackay et al., 2021). Hybridization between ‘East Africa’ and ‘Nepal’ or
618 ‘Southern Africa’ accessions may also generate useful genetic variation for use in the genetically
619 narrow East Africa region. A study of *Eleusine* germplasm panels containing known and putative
620 crop wild progenitors is required to understand the crop’s demographic history further. In our
621 ongoing research, we seek to understand the nature and extent of genotype-by-environment
622 interactions in finger millet, to guide whether more local germplasm panels would be better suited
623 for GWAS, and to assess the prospects for climate change adaption of the crop. As genomic
624 resources continue to develop for finger millet, breeding material selection approaches that assign
625 genomic estimated breeding values to each separate sub-genome also open a possibility for
626 weighted sub-genome selection (Santantonio et al., 2019).

627 **ACKNOWLEDGEMENTS**

628 The authors are thankful for helpful comments from Ian Mackay and Rajiv Sharma, and
629 technical assistance from Ann Murithi and Erick Owuor Mikwa. We also thank Peter Bradbury

630 for adding a bespoke filtering option in TASSEL for removing SNPs with a heterozygosity level
631 greater than $2pq \times (1 - F)$.

632 **AUTHOR CONTRIBUTIONS**

633 JB, IKD and DAO conceptualized the study. HFO coordinated the collection of field phenotype
634 data. DAO coordinated the generation and initial screening of molecular marker data. SMJ carried
635 out genomic DNA extractions of the 458 samples. JB conducted further data screening and all
636 statistical analyses. IKD, RCG, JBu, GG and DAO contributed to determining appropriate analysis
637 methods and interpreting findings. JB and IKD wrote the first draft of the paper that was then
638 contributed to by all other authors.

639 **CONFLICT OF INTEREST**

640 The authors declare no conflict of interest.

641 **SUPPLEMENTAL MATERIAL**

642 **Supplemental File S1** contains supplemental tables (**Tables S2,5,6**) and figures (**Figs. S1-13**).
643 **Supplemental File S2** contains supplemental **Tables S1,3,4,7,8**.

644 **FUNDING**

645 SRUC authors are grateful for Global Challenge Research Funding on orphan crops (project
646 BB/P022537/1: Formulating Value Chains for Orphan Crops in Africa, 2017-2019, Foundation
647 Award for Global Agriculture and Food Systems). JB was funded through an SRUC studentship
648 Research Excellence Grant.

649

DATA AVAILABILITY

650 All data generated and analyzed during this study are included in this published article and its
651 supplemental material. The raw phenotypic and DArTseq SNP data were deposited into Dryad
652 Digital Repository (<http://datadryad.org/>).

653

REFERENCES

- 654 Arya, L., Verma, M., Gupta, V. K., & Seetharam, A. (2013). Use of genomic and genic SSR
655 markers for assessing genetic diversity and population structure in Indian and African finger
656 millet (*Eleusine coracana* (L.) Gaertn.) germplasm. *Plant Systematics and Evolution*,
657 299(7), 1395–1401. <https://doi.org/10.1007/s00606-013-0822-x>
- 658 Babu, B. K., Sood, S., Chandrashekara, C., Pattanayak, A., & Kant, L. (2018). Mapping
659 quantitative trait loci for important agronomic traits in finger millet (*Eleusine coracana*)
660 mini core collection with genomic and genic SSR markers. *Journal of Plant Biochemistry
661 and Biotechnology*, 27(4), 401–414. <https://doi.org/10.1007/s13562-018-0449-7>
- 662 Bančić, J., Werner, C., Gaynor, C., Gorjanc, G., Odeny, D., Ojulong, H. F., ... Hickey, J. M.
663 (2021). Modelling illustrates that genomic selection provides new opportunities for
664 intercrop breeding. *Frontiers in Plant Science*, 12, 1–16.
665 <https://doi.org/10.1101/2020.09.11.292912>
- 666 Bharathi, A. (2011). *Phenotypic and genotypic diversity of global finger millet (Eleusine
667 coracana (L.) Gaertn.) composite collection*. Tamil Nadu Agricultural University.
- 668 Bradbury, P. J., Zhang, Z., Kroon, D. E., Casstevens, T. M., Ramdoss, Y., & Buckler, E. S.
669 (2007). TASSEL: Software for association mapping of complex traits in diverse samples.
670 *Bioinformatics*, 23(19), 2633–2635. <https://doi.org/10.1093/bioinformatics/btm308>
- 671 Brinton, J., & Uauy, C. (2019). A reductionist approach to dissecting grain weight and yield in
672 wheat. *Journal of Integrative Plant Biology*, 61(3), 337–358.
673 <https://doi.org/10.1111/jipb.12741>
- 674 Brooker, R. W., Jones, H. G., Paterson, E., Watson, C., Brooker, R. W., Bennett, A. E., ...
675 McKenzie, B. M. (2015). Improving intercropping : a synthesis of research in agronomy ,
676 plant physiology and Research review Improving intercropping : a synthesis of research in
677 agronomy , plant physiology and ecology. *New Phytologist*, 206(APRIL), 107–117.
- 678 Butler, D. G., Cullis, B. R., Gilmour, A. R., Gogel, B. J., & Thompson, R. (2017). ASReml-R
679 Reference Manual Version 4. *ASReml-R Reference Manual*, 176. Retrieved from
680 [https://asreml.kb.vsnr.co.uk/wp-content/uploads/sites/3/2018/02/ASReml-R-Reference-
681 Manual-4.pdf](https://asreml.kb.vsnr.co.uk/wp-content/uploads/sites/3/2018/02/ASReml-R-Reference-
681 Manual-4.pdf)
- 682 Danecek, P., Auton, A., Abecasis, G., Albers, C. A., Banks, E., DePristo, M. A., ... Durbin, R.

- 683 (2011). The variant call format and VCFtools. *Bioinformatics*, 27(15), 2156–2158.
684 <https://doi.org/10.1093/bioinformatics/btr330>
- 685 Dawson, I. K., Powell, W., Hendre, P., Bančić, J., Hickey, J. M., Kindt, R., ... Jamnadass, R.
686 (2019). The role of genetics in mainstreaming the production of new and orphan crops to
687 diversify food systems and support human nutrition. *New Phytologist*.
688 <https://doi.org/10.1111/nph.15895>
- 689 de Wet, J. M. J., Prasada Rao, K. E., Brink, D. E., & Mengesha, M. H. (1984). Systematics and
690 Evolution of Eleusine coracana (Gramineae). *American Journal of Botany*, 71(4), 550–
691 557.
- 692 Dida, M. M., & Devos, K. M. (2006). Finger Millet. *Cereals and Millets*, 1, 333–343.
- 693 Dida, M. M., Oduori, C. A., Manthi, S. J., Avosa, M. O., Mikwa, E. O., Ojulong, H. F., &
694 Odeny, D. A. (2021). Novel sources of resistance to blast disease in finger millet. *Crop*
695 *Science*, 61(1), 250–262. <https://doi.org/10.1002/csc2.20378>
- 696 Dida, M. M., Wanyera, N., Harrison Dunn, M. L., Bennetzen, J. L., & Devos, K. M. (2008).
697 Population Structure and Diversity in Finger Millet (*Eleusine coracana*) Germplasm.
698 *Tropical Plant Biology*, 1(2), 131–141. <https://doi.org/10.1007/s12042-008-9012-3>
- 699 Dray, S., & Dufour, A. B. (2007). The ade4 package: Implementing the duality diagram for
700 ecologists. *Journal of Statistical Software*, 22(4), 1–20.
701 <https://doi.org/10.18637/jss.v022.i04>
- 702 Endelman, J. B., & Jannink, J. L. (2012). Shrinkage estimation of the realized relationship
703 matrix. *G3: Genes, Genomes, Genetics*, 2(11), 1405–1413.
704 <https://doi.org/10.1534/g3.112.004259>
- 705 Feldman, M., & Levy, A. A. (2012). Genome evolution due to allopolyploidization in wheat.
706 *Genetics*, 192(3), 763–774. <https://doi.org/10.1534/genetics.112.146316>
- 707 Flint-Garcia, S. A., Thornsberry, J. M., & Edwards, S. B. (2003). Structure of Linkage
708 Disequilibrium in Plants. *Annual Review of Plant Biology*, 54, 357–374.
709 <https://doi.org/10.1146/annurev.arplant.54.031902.134907>
- 710 Gimode, D., Odeny, D. A., De Villiers, E. P., Wanyonyi, S., Dida, M. M., Mneney, E. E., ... De
711 Villiers, S. M. (2016). Identification of SNP and SSR markers in finger millet using next
712 generation sequencing technologies. *PLoS ONE*, 11(7), 1–23.
713 <https://doi.org/10.1371/journal.pone.0159437>
- 714 Goudet, J. (2005). HIERFSTAT, a package for R to compute and test hierarchical F-statistics.
715 *Molecular Ecology Notes*, 5, 184–186. <https://doi.org/10.1111/j.1471-8278>
- 716 Hatakeyama, M., Aluri, S., Balachandran, M. T., Sivarajan, S. R., Patrignani, A., Grüter, S., ...
717 Shimizu, K. K. (2018). Multiple hybrid de novo genome assembly of finger millet, an
718 orphan allotetraploid crop. *DNA Research*, 25(1), 39–47.
719 <https://doi.org/10.1093/dnares/dsx036>

- 720 He, F., Pasam, R., Shi, F., Kant, S., Keeble-Gagnere, G., Kay, P., ... Akhunov, E. (2019). Exome
721 sequencing highlights the role of wild-relative introgression in shaping the adaptive
722 landscape of the wheat genome. *Nature Genetics*, *51*(5), 896–904.
723 <https://doi.org/10.1038/s41588-019-0382-2>
- 724 Hill, W. G., & Weir, B. S. (1988). Variances and covariances of squared linkage disequilibria in
725 finite populations. *Theoretical Population Biology*, *33*(1), 54–78.
726 [https://doi.org/10.1016/0040-5809\(88\)90004-4](https://doi.org/10.1016/0040-5809(88)90004-4)
- 727 Hilu, K. W., & de Wet, J. M. J. (1976). Domestication of *Eleusine coracana*. *Economic Botany*,
728 *30*(3), 199–208. Retrieved from <https://www.jstor.org/stable/4253732>
- 729 Hittalmani, S., Mahesh, H. B., Shirke, M. D., Biradar, H., Uday, G., Aruna, Y. R., ... Mohanrao,
730 A. (2017). Genome and Transcriptome sequence of Finger millet (*Eleusine coracana* (L.)
731 Gaertn.) provides insights into drought tolerance and nutraceutical properties. *BMC*
732 *Genomics*, *18*(1), 1–16. <https://doi.org/10.1186/s12864-017-3850-z>
- 733 Jaiswal, V., Gupta, S., Gahlaut, V., Muthamilarasan, M., Bandyopadhyay, T., Ramchiary, N., &
734 Prasad, M. (2019). Genome-Wide Association Study of Major Agronomic Traits in Foxtail
735 Millet (*Setaria italica* L.) Using ddRAD Sequencing. *Scientific Reports*, *9*(1), 3–5.
736 <https://doi.org/10.1038/s41598-019-41602-6>
- 737 Jamnadass, R., Mumm, R. H., Hale, I., Hendre, P., Muchugi, A., Dawson, I. K., ... Van Deynze,
738 A. (2020). Enhancing African orphan crops with genomics. *Nature Genetics*, *52*(4), 356–
739 360. <https://doi.org/10.1038/s41588-020-0601-x>
- 740 Jombart, T. (2008). Adegnet: A R package for the multivariate analysis of genetic markers.
741 *Bioinformatics*, *24*(11), 1403–1405. <https://doi.org/10.1093/bioinformatics/btn129>
- 742 Kamenya, S. N., Mikwa, E. O., Song, B., & Odeny, D. A. (2021). Genetics and breeding for
743 climate change in Orphan crops. *Theoretical and Applied Genetics*, 1–29.
744 <https://doi.org/10.1007/s00122-020-03755-1>
- 745 Kassambara, A., & Mundt, F. (2020). factoextra: Extract and Visualize the Results of
746 Multivariate Data Analyses. Retrieved from <https://cran.r-project.org/package=factoextra>
- 747 Komsta, L., & Novomestky, F. (2011). Package ‘moments,’ 1–15.
- 748 Kooke, R., Kruijer, W., Bours, R., Becker, F., Kuhn, A., van de Geest, H., ... Keurentjes, J. J. B.
749 (2016). Genome-wide association mapping and genomic prediction elucidate the genetic
750 architecture of morphological traits in arabidopsis. *Plant Physiology*, *170*(4), 2187–2203.
751 <https://doi.org/10.1104/pp.15.00997>
- 752 Kozak, M., Bocianowski, J., Liersch, A., Tartanus, M., Bartkowiak-Broda, I., Piotto, F. A., &
753 Azevedo, R. A. (2011). Genetic divergence is not the same as phenotypic divergence.
754 *Molecular Breeding*, *28*(2), 277–280. <https://doi.org/10.1007/s11032-011-9583-9>
- 755 Labroo, M. R., Studer, A. J., & Rutkoski, J. E. (2021). Heterosis and Hybrid Crop Breeding : A
756 Multidisciplinary Review, *12*(February), 1–19. <https://doi.org/10.3389/fgene.2021.643761>

- 757 Levy, A. A., & Feldman, M. (2002). The impact of polyploidy on grass genome evolution. *Plant*
758 *Physiology*, 130(4), 1587–1593. <https://doi.org/10.1104/pp.015727>
- 759 Liu, Q., Jiang, B., Wen, J., & Peterson, P. M. (2014). Low-copy nuclear gene and McGISH
760 resolves polyploid history of eleusine coracana and morphological character evolution in
761 Eleusine. *Turkish Journal of Botany*, 38(1), 1–12. <https://doi.org/10.3906/bot-1305-12>
- 762 Lule, D., De Villiers, S., Fetene, M., Odeny, D. A., Rathore, A., Das, R. R., & Tesfaye, K.
763 (2018). Genetic diversity and association mapping of Ethiopian and exotic finger millet
764 accessions. *Crop and Pasture Science*, 69(9), 879–891. <https://doi.org/10.1071/CP18175>
- 765 Mackay, I. J., Cockram, J., Howell, P., & Powell, W. (2021). Understanding the classics: the
766 unifying concepts of transgressive segregation, inbreeding depression and heterosis and
767 their central relevance for crop breeding. *Plant Biotechnology Journal*, 19(1), 26–34.
768 <https://doi.org/10.1111/pbi.13481>
- 769 Mangin, B., Siberchicot, A., Nicolas, S., Doligez, A., This, P., & Cierco-Ayrolles, C. (2012).
770 Novel measures of linkage disequilibrium that correct the bias due to population structure
771 and relatedness. *Heredity*, 108(3), 285–291. <https://doi.org/10.1038/hdy.2011.73>
- 772 Manyasa, E. O., Tongoona, P., Shanahan, P., Mgonja, M. A., & De Villiers, S. (2015). Genetic
773 diversity in East African finger millet (*Eleusine coracana* (L.) Gaertn) landraces based on
774 SSR markers and some qualitative traits. *Plant Genetic Resources: Characterization and*
775 *Utilization*, 13(1), 45–55. <https://doi.org/10.1017/S1479262114000628>
- 776 Manyasa Okuku, E., Tongoona, P., Shanahan, P., Githiri, M., & Rathore, A. (2016).
777 Correlations, path coefficient analysis and heritability for quantitative traits in finger millet
778 landraces. *Philippine Journal of Science*, 145(2), 197–208.
- 779 Marroni, F., Pinosio, S., Zaina, G., Fogolari, F., Felice, N., Cattonaro, F., & Morgante, M.
780 (2011). Nucleotide diversity and linkage disequilibrium in *Populus nigra* cinnamyl alcohol
781 dehydrogenase (CAD4) gene. *Tree Genetics and Genomes*, 7(5), 1011–1023.
782 <https://doi.org/10.1007/s11295-011-0391-5>
- 783 Meyer, R. S., & Purugganan, M. D. (2013). Evolution of crop species: Genetics of domestication
784 and diversification. *Nature Reviews Genetics*, 14(12), 840–852.
785 <https://doi.org/10.1038/nrg3605>
- 786 Mirza, N., & Marla, S. S. (2019). Finger Millet (*Eleusine coracana* L. Gaertn.) Breeding. In J. M.
787 Al-Khayri, S. M. Jain, & D. V Johnson (Eds.), *Advances in Plant Breeding Strategies:*
788 *Cereals: Volume 5* (pp. 83–132). Cham: Springer International Publishing.
789 https://doi.org/10.1007/978-3-030-23108-8_3
- 790 Mustafa, M. A., Mayes, S., & Massawe, F. (2019). Crop Diversification Through a Wider Use of
791 Underutilized Crops: A Strategy to Ensure Food and Nutrition Security in the Face of
792 Climate Change. In A. Sarkar, S. R. Sensarma, & G. W. vanLoon (Eds.), *Sustainable*
793 *Solutions for Food Security : Combating Climate Change by Adaptation* (pp. 125–149).
794 Cham: Springer International Publishing. https://doi.org/10.1007/978-3-319-77878-5_7

- 795 Nei, M., & Li, W. H. (1979). Mathematical model for studying genetic variation in terms of
796 restriction endonucleases. *Proceedings of the National Academy of Sciences of the United*
797 *States of America*, 76(10), 5269–5273. <https://doi.org/10.1073/pnas.76.10.5269>
- 798 Nei, Masatoshi. (1973). Analysis of Gene Diversity in Subdivided Populations. *Proceedings of*
799 *the National Academy of Sciences of the United States of America*, 70(12), 3321–3323.
800 <https://doi.org/10.1073/pnas.70.12.3321>
- 801 Odeny, D. A., Niazi, A., Tesfaye, K., Lule, D., Wanyonyi, S., & Kunguni, J. S. (2020). Genomic
802 Designing for Climate Smart Finger Millet. In C. Kole (Ed.), *Genomic Designing of*
803 *Climate-Smart Cereal Crops* (pp. 287–307). Cham: Springer International Publishing.
804 https://doi.org/10.1007/978-3-319-93381-8_7
- 805 Pandian, S., Satish, L., Rameshkumar, R., Muthuramalingam, P., Rency, A. S., Rathinapriya, P.,
806 & Ramesh, M. (2018). Analysis of population structure and genetic diversity in an exotic
807 germplasm collection of *Eleusine coracana* (L.) Gaertn. using genic-SSR markers. *Gene*,
808 653(February), 80–90. <https://doi.org/10.1016/j.gene.2018.02.018>
- 809 Paradis, E. (2010). Pegas: An R package for population genetics with an integrated-modular
810 approach. *Bioinformatics*, 26(3), 419–420. <https://doi.org/10.1093/bioinformatics/btp696>
- 811 Pearson, K. (1895). VII. Note on regression and inheritance in the case of two parents.
812 *Proceedings of the Royal Society*, 58, 240–242. Retrieved from
813 <http://doi.org/10.1098/rspl.1895.0041>
- 814 Pickrell, J. K., & Pritchard, J. K. (2012). Inference of Population Splits and Mixtures from
815 Genome-Wide Allele Frequency Data. *PLoS Genetics*, 8(11).
816 <https://doi.org/10.1371/journal.pgen.1002967>
- 817 Puranik, S., Sahu, P. P., Beynon, S., & Srivastava, R. K. (2020). Genome-wide association
818 mapping and comparative genomics identifies genomic regions governing grain nutritional
819 traits in finger millet (*Eleusine coracana* L . Gaertn .). *Plants People Planet*, (July), 1–14.
820 <https://doi.org/10.1002/ppp3.10120>
- 821 Qi, P., Gimode, D., Saha, D., Schröder, S., Chakraborty, D., Wang, X., ... Devos, K. M. (2018).
822 UGbS-Flex, a novel bioinformatics pipeline for imputation-free SNP discovery in
823 polyploids without a reference genome: Finger millet as a case study. *BMC Plant Biology*,
824 18(1), 1–19. <https://doi.org/10.1186/s12870-018-1316-3>
- 825 R Core Team. (2019). R: A Language and Environment for Statistical Computing. Vienna,
826 Austria. Retrieved from <https://www.r-project.org/>
- 827 Ramakrishnan, M., Antony Ceasar, S., Duraipandiyam, V., Al-Dhabi, N. A., & Ignacimuthu, S.
828 (2016). Assessment of genetic diversity, population structure and relationships in Indian and
829 non-Indian genotypes of finger millet (*Eleusine coracana* (L.) Gaertn) using genomic SSR
830 markers. *SpringerPlus*, 5(1), 1–11. <https://doi.org/10.1186/s40064-015-1626-y>
- 831 Rao, S. A. (1980). *Germplasm collecting mission to Zambia*. Patancheru, Andhra Pradesh, India.
832 Retrieved from <http://eprints.icrisat.ac.in/id/eprint/4229>

- 833 Robinson, J. T., Thorvaldsdóttir, H., Winckler, W., Guttman, M., Lander, E. S., Getz, G., &
834 Mesirov, J. P. (2011). Integrative Genome Viewer. *Nature Biotechnology*, 29(1), 24–26.
835 <https://doi.org/10.1038/nbt.1754>. Integrative
- 836 Rodríguez, G. R., Muñoz, S., Anderson, C., Sim, S. C., Michel, A., Causse, M., ... van der
837 Knaap, E. (2011). Distribution of SUN, OVATE, LC, and FAS in the tomato germplasm
838 and the relationship to fruit shape diversity. *Plant Physiology*, 156(1), 275–285.
839 <https://doi.org/10.1104/pp.110.167577>
- 840 Saitou, N., & Nei, M. (1987). The neighbor-joining method: a new method for reconstructing
841 phylogenetic trees. *Molecular Biology and Evolution*, 4(4), 406–425.
842 <https://doi.org/10.1093/oxfordjournals.molbev.a040454>
- 843 Sansaloni, C., Petrolì, C., Jaccoud, D., Carling, J., Detering, F., Grattapaglia, D., & Kilian, A.
844 (2011). Diversity Arrays Technology (DArT) and next-generation sequencing combined:
845 genome-wide, high throughput, highly informative genotyping for molecular breeding of
846 Eucalyptus. *BMC Proceedings*, 5(S7). <https://doi.org/10.1186/1753-6561-5-s7-p54>
- 847 Santantonio, N., Jannink, J. L., & Sorrells, M. (2019). Prediction of subgenome additive and
848 interaction effects in allohexaploid wheat. *G3: Genes, Genomes, Genetics*, 9(3), 685–698.
849 <https://doi.org/10.1534/g3.118.200613>
- 850 Schliep, K. P. (2011). phangorn: Phylogenetic analysis in R. *Bioinformatics*, 27(4), 592–593.
851 <https://doi.org/10.1093/bioinformatics/btq706>
- 852 Sharma, D., Tiwari, A., Sood, S., Jamra, G., Singh, N. K., Meher, P. K., & Kumar, A. (2018).
853 Genome wide association mapping of agro-morphological traits among a diverse collection
854 of finger millet (*Eleusine coracana* L.) genotypes using SNP markers. *PLoS ONE*, 13(8), 1–
855 21. <https://doi.org/10.1371/journal.pone.0199444>
- 856 Sood, S., Joshi, D. C., Chandra, A. K., & Kumar, A. (2019). Phenomics and genomics of finger
857 millet: current status and future prospects. *Planta*, 250(3), 731–751.
858 <https://doi.org/10.1007/s00425-019-03159-6>
- 859 Sood, S., Kumar, A., Kalyana Babu, B., Gaur, V. S., Pandey, D., Kant, L., & Pattanayak, A.
860 (2016). Gene discovery and advances in finger millet [*Eleusine coracana* (L.) Gaertn.]
861 genomics-an important nutri-cereal of future. *Frontiers in Plant Science*, 7, 1–17.
862 <https://doi.org/10.3389/fpls.2016.01634>
- 863 South, A. (2011). rworldmap: A new R package for mapping global data. *R Journal*, 3(1), 35–43.
864 <https://doi.org/10.32614/rj-2011-006>
- 865 Stebbins, G. L. (1950). *Variation and Evolution in Plants* (p. 644). Boston, MA: Columbia
866 University Press. <https://doi.org/10.7312/steb94536>
- 867 Tiwari, A., Sharma, D., Sood, S., Jaiswal, J. P., Pachauri, S. P., Ramteke, P. W., & Kumar, A.
868 (2020). Genome-wide association mapping for seed protein content in finger millet
869 (*Eleusine coracana*) global collection through genotyping by sequencing. *Journal of Cereal*
870 *Science*, 91(May 2019), 102888. <https://doi.org/10.1016/j.jcs.2019.102888>

- 871 Upadhyaya, H. D., Gowda, C. L. L., Pundir, R. P. S., Reddy, V. G., & Singh, S. (2006).
872 Development of core subset of finger millet germplasm using geographical origin and data
873 on 14 quantitative traits. *Genetic Resources and Crop Evolution*, 53(4), 679–685.
874 <https://doi.org/10.1007/s10722-004-3228-3>
- 875 von Grebmer, K., Saltzman, A., Birol, E., Wiesmann, D., Prasai, N., Yin, S., ... Menon, P.
876 (2014). *2014 Global Hunger Index: The Challenge of Hidden Hunger*. Bonn, Washington,
877 D.C., and Dublin: Welthungerhilfe, International Food Policy Research Institute, and
878 Concern Worldwide. Retrieved from <http://dx.doi.org/10.2499/9780896299580>
- 879 Weir, B. S., & Cockerham, C. C. (1984). Estimating F-statistics for the analysis of population
880 structure. *Evolution*, 38(6), 1358–1370. <https://doi.org/10.1111/j.1558-5646.1984.tb05657.x>
- 881 Wickham, H. (2009). *ggplot2: elegant graphics for data analysis*. Springer New York. Retrieved
882 from <http://had.co.nz/ggplot2/book>
- 883 Yu, J., Pressoir, G., Briggs, W. H., Bi, I. V., Yamasaki, M., Doebley, J. F., ... Buckler, E. S.
884 (2006). A unified mixed-model method for association mapping that accounts for multiple
885 levels of relatedness. *Nature Genetics*, 38(2), 203–208. <https://doi.org/10.1038/ng1702>
- 886 Zhang, H., Hall, N., Goertzen, L. R., Chen, C. Y., Peatman, E., Patel, J., & Scott McElroy, J.
887 (2019). Transcriptome analysis reveals unique relationships among eleusine species and
888 heritage of eleusine coracana. *G3: Genes, Genomes, Genetics*, 9(6), 2029–2036.
889 <https://doi.org/10.1534/g3.119.400214>
- 890